

HIGH-FIELD COMBINED-FUNCTION MAGNETS FOR A 1.5×1.5 TeV MUON COLLIDER STORAGE RING*

V.V. Kashikhin[#], Y.I. Alexahin, N.V. Mokhov, A.V. Zlobin, Fermilab, Batavia, IL 60510, USA

Abstract

Designs and parameters of dipoles and combined-function quadrupoles for bending arc lattice of a 1.5×1.5 TeV muon collider with an average luminosity of $4 \times 10^{34} \text{ cm}^{-2}\text{s}^{-1}$ are presented. The magnets use the Nb₃Sn superconductor and provide the required gradients and fields with the appropriate operating margins and field quality. The magnet apertures accommodate tungsten liners to minimize the dynamic heat load in the superconducting coils.

INTRODUCTION

Operating conditions pose significant challenges to superconducting (SC) magnets used in a Muon Collider Storage Ring (MCSR). Dipole magnets have to provide a high magnetic field to reduce the ring circumference and thus maximize the number of muon collisions during their lifetime. Moreover, SC coils need to be protected from showers induced by the decay electrons since about one third of the muon beam energy or an average of ~1 kW/m is deposited along the ring by such showers. The high operating fields and large heat depositions require using advanced SC materials such as Nb₃Sn and advanced magnet technologies.

The high level and distribution of heat deposition in MCSR [1, 2] requires either large aperture magnets to accommodate thick high-Z absorbers to protect the SC coils or an open midplane (OM) design to create a pass for the decay electrons to high-Z absorbers placed outside the coils. Both magnet designs were carefully analyzed [3, 4]. In spite of the attractiveness of the OM approach, the analysis revealed serious issues for this magnet type. Besides the structural issues related to handling the large vertical forces in the coils with OM gaps, the dynamic heat load in the OM dipoles is still large even after implementation of appropriate protective measures [5].

As shown in [5], the dynamic heat load to cold mass is about 25 W/m in the 0.75×0.75 TeV MCSR since the decay electrons have a too large transverse momentum to pass through the open mid-plane with a strong vertical defocusing quadrupole field in the gap. Thus, a large aperture and an internal absorber are also needed for the OM magnets. Furthermore, for the muon beam energies of 1.5 TeV or higher, a dipole component is needed in the quadrupoles to mitigate the neutrino radiation problem [6]. It suggests using combined-function quadrupoles with the dipole field components. Achieving the required level of both quadrupole and dipole components in OM combined-function magnets has serious challenges.

This paper presents the design study of the bending arc magnets of a 1.5×1.5 TeV MCSR with an average luminosity of $4 \times 10^{34} \text{ cm}^{-2}\text{s}^{-1}$ based on the relevant [7] lattice and an internal absorber.

MCSR MAGNET REQUIREMENTS

Target parameters of the MCSR are shown in Table 1. The arc cell lattice and variations of horizontal and vertical beta-functions and dispersion [7] are shown in Fig.1 (top). The lattice consists of strong bending dipoles and combined-function quadrupoles with large dipole fields. Horizontal (*x*) and vertical (*y*) beam size variations (4σ) in the arc magnets are shown in Fig. 1 (bottom). The aperture of the magnets is determined by the following criterion $D_{x,y} = 8\sigma_{\text{max}}$ [7].

Table 2 shows the ranges of dipole field *B*, field gradient *G* and beam aperture $D_{x,y}$ for the combined - function defocusing (QDA) and focusing (QFA) quadrupoles, and bending dipoles (D).

The main goal of this study was to determine possibilities and limitations to achieve the operating gradient and field of 85 T/m and 8 T with ~20 % margin at 4.5 K in the arc magnets with a beam aperture of $5.6 \times 0.2 \text{ cm}^2$ and an inner absorber (liner).

Table 1: MC Storage Ring Parameters

Parameter	Unit	Value
Beam energy	TeV	1.5
Circumference	km	4.5
Momentum acceptance	%	±0.5
Transverse emittance, ϵ_N	$\pi \cdot \text{mm} \cdot \text{mrad}$	25
Number of IPs		2
β^*	cm	0.5

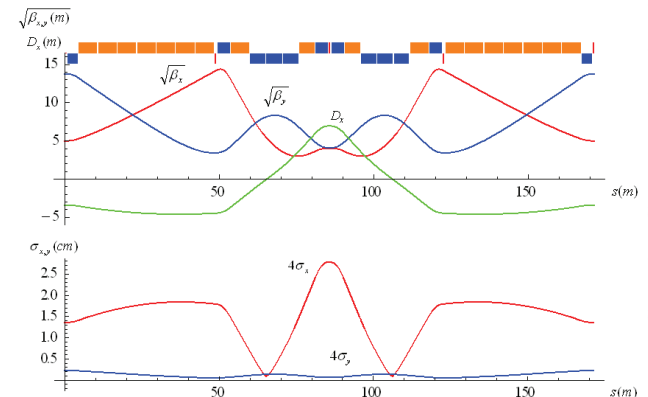


Figure 1: MC arc cell concept and beam size in magnets.

Table 2: MCSR Magnet Target Parameters

Magnet	G (T/m)	B (T)	D_x (cm)	D_y (cm)
QDA1/3	-(31-35)	9.0	2.8	0.3-0.5
QFA2/4	85	8.0	3.6-5.6	0.2
D	-	10.4	3.7-4.8	0.2-0.4

* Work supported by Fermi Research Alliance, LLC, under contract No. DE-AC02-07CH11359 with the U.S. Department of Energy
[#] vadim@fnal.gov

MAGNET DESIGNS AND PARAMETERS

Internal Absorber and Magnet Aperture

Magnet apertures have to provide an adequate space for the internal absorber, vacuum insulation, magnet cold bore, and helium channel. The internal absorber geometry and size were estimated based on the MARS-calculated azimuthal distributions of heat deposition in MCSR and the target attenuation factor of 100 to keep the average dynamic heat load in SC magnets below 10 W/m.

Fig. 2 shows the azimuthal distribution of power density in the collider arc for tungsten absorbers of various thicknesses inside the magnet aperture for one 2 TeV muon beam [1, 2]. The power which penetrates tungsten shields for 2 TeV and 0.05 TeV muon beams as a function of shield thickness is shown in Fig. 3 [2].

Taking into account that the quench limit of Nb₃Sn coil at 80 % of its critical current is ~5 mW/g [8], and assuming a factor of 3 safety margin, the minimum absorber thickness to keep the heat deposition in Nb₃Sn coil below 1.5-1.7 mW/g is only ~2 cm (Fig. 2). However, to keep the heat load in MCSR magnets below 10 W/m the minimum absorber thickness increases to ~5 cm (Fig. 3). It is a conservative assumption since the Figs. 2 and 3 were calculated without tungsten masks in between the magnets, which demonstrated to be highly efficient in reducing the heat deposition in magnets [5].

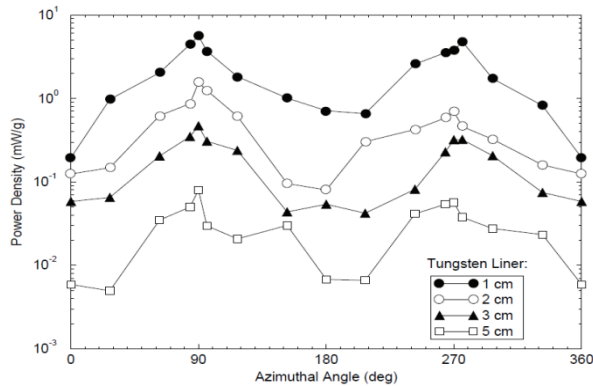


Figure 2: Azimuthal distribution of power density in the collider arc for different inner tungsten absorbers [1, 2].

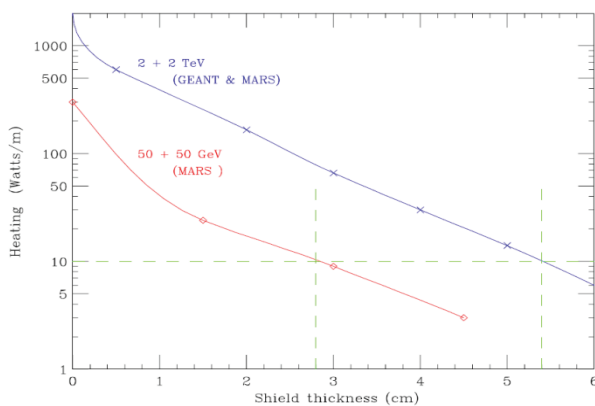


Figure 3: Power penetrating tungsten shields vs. shield thickness for 2 TeV and 0.05 TeV muon beams [2].

The strong azimuthal dependence of the power density in MCSR suggests using an absorber with a variable azimuthal thickness. In this study, an asymmetric elliptical absorber with 5 cm (inwards the ring) and 3 cm (outwards the ring) horizontal thicknesses has been chosen. Assuming a round magnet aperture, its diameter is determined by the horizontal beam size of 56 mm and the total horizontal absorber thickness of 80 mm, 5 mm vacuum gaps, 2 mm thick He pipe, and 2 mm annular He channel on each side. The coil ID in further analysis was rounded to 150 mm. The selected absorber size, geometry and magnet aperture will be optimized during the radiation heat deposition modeling.

The beam center shift with respect to the coil center is ~10 mm. Thus, the radius of the good field quality region is 38 mm or a half of the coil inner radius. Free space between the elliptical absorber and the cold bore can be used for absorber support and cooling systems. MCSR magnets with elliptical aperture are discussed in [9].

Magnet Designs and Parameters

The level of fields in MCSR magnets and the operating temperature calls for the Nb₃Sn superconductor. Nb₃Sn strand and coil technology has advanced over the last decade that reliable magnets can be fabricated. Parameters of the considered Nb₃Sn strand and Rutherford cable are presented in Table 3.

The magnet designs are based on 2-layer dipole and quadrupole coils with 150 mm apertures, shown in Fig. 4, and the cold iron yoke. The main magnet parameters are listed in Table 4. The coil cross-sections were optimized to achieve the necessary field level at 4.5 K and a good field quality in the area occupied by beams using ROXIE code [10].

The dipole and quadrupole coils in the combined-function magnets are powered independently.

Table 3: Cable Parameters

Parameter	Value
Number of strands	40
Strand diameter (mm)	1.0
Cu/nonCu ratio	1.0
SSL J _c (12T, 4.2K) (A/mm ²)	3000
Cable mid-thickness (mm)	1.81
Cable keystone angle (deg)	0.88-1.00
Cable width (mm)	20.59
Cable insulation	0.20

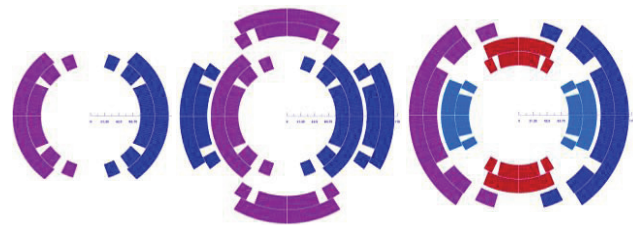


Figure 4: Bending dipole (left) and combined-function quadrupoles with the dipole coil inside (center) and outside (right) of the main quadrupole coil. The color shades represent the current directions in the coils.

Table 4: Parameters of Arc Dipole and Combined-Function Quadrupole at $T_{op}=4.5$ K

Parameter	Arc dipole	D/Q	Q/D	
	D	QDA1/3	QDA1/3	QFA2/4
Maximum field in coil (T)*	15.7	16.8/16.7	16.5/17.5	
Maximum field or gradient in aperture (T or T/m)*	14.4	9.3/76.7	12.0/72.5	
Operating field or gradient in aperture (T or T/m)*	10.4	9.0/35.0	9.0/35.0	8.0/85.0
Fraction of SSL at the operating field*	0.72	0.75/0.61	0.70/0.64	0.75/0.86
Inductance L_{self} (mH/m)*	18.2	16.0/20.6	44.2/6.9	
Stored energy E at the operating field (MJ/m)*	1.7	1.5/0.5	2.9/0.1	2.3/0.6
Horizontal Lorentz force F_x at the operating field (MN/m)*#	5.8	7.7/-0.1	7.2/2.2	6.1/5.5
Vertical Lorentz force F_y at the operating field (MN/m)*#	-2.4	-4.5/-1.6	-4.0/-0.3	-4.5/-1.5

* the first value is for dipole coils, the second one is for quadrupole coils; # totals per 1st quadrant in dipole and per 1st octant in quadrupole.

As can be seen from Table 4, the arc dipole provides the 10.4 T field with a large margin that can be used to optimize the space between dipoles for tungsten masks.

The combined-function quadrupole was designed using two approaches: by placing a main quadrupole coil around the 150-mm arc dipole coil (D/Q); and by placing the dipole coil around the 150-mm main quadrupole coil (Q/D). A 5-mm spacer separated the dipole and quadrupole coils; the iron yoke was 10 mm from the coil.

Both combined-function magnets have nearly the same conductor volume, but the Q/D design has a superior performance: ~30 % higher dipole field and about the same gradient as in the D/Q case. Since the D/Q configuration does not meet the QFA requirements with reasonable margins, it is not shown for these magnets. Field distribution in the Q/D case is shown in Fig. 5 at the maximum current in both coils.

Geometrical field harmonics for the arc dipole and combined-function quadrupole of both designs are shown in Table 5. All the low-order harmonics in the beam area are less than 10^{-4} of the main field component.

Table 5: Geometrical harmonics at $R_{ref}=50$ mm (10^{-4})

Harmonic #	Dipole	CF Quadrupole	
		D/Q	Q/D
b_3	-0.23	0.39	0.03
b_5	-0.16	0.28	0.07
b_6	-	0.16	-0.09
b_7	-0.48	0.92	0.58
b_9	0.16	0.12	-0.01
b_{10}	-	-0.01	0.05

CONCLUSION

Arc magnets for a 1.5×1.5 TeV MCSR with an average luminosity of $4 \times 10^{34} \text{ cm}^{-2}\text{s}^{-1}$ based on the Nb₃Sn Rutherford cables have been studied. The magnets have a 150 mm aperture, work at 4.5 K and provide the necessary operating field/gradient with adequate margins and accelerator-quality field. Together with the magnets for 1.5×1.5 TeV MCSR Interaction Regions [11], they advance the understanding of the challenges and limitations for the Muon Collider magnets.

The maximum field in the coils reaches ~17 T, which is the practical limit for the Nb₃Sn magnets of this type. Using hybrid HTS/LTS coils to increase the operating field is hypothetically possible with HTS inserts. However, in the combined-function quadrupoles, it would require the expensive HTS in a large fraction of coil.

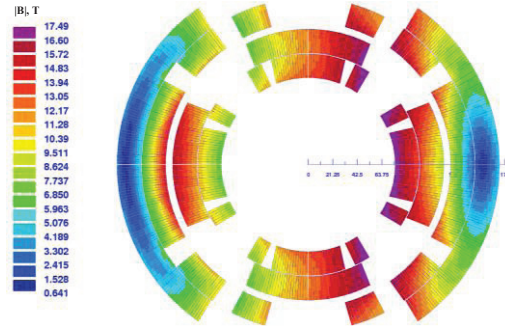


Figure 5: Field distribution in the Q/D coil cross-section.

REFERENCES

- [1] C.J. Johnstone and N.V. Mokhov, Proc. of the DPF/DPB Summer Study on High-Energy Physics, p. 226; FERMILABConf-96-366, 1996.
- [2] C.M. Ankenbrandt et al., "Status of muon collider research and development and future plans," PRST-AB 2 (1999) 081001.
- [3] A.V. Zlobin et al., "Magnet Designs for Muon Collider Ring and Interaction Regions," IPAC'10, Kyoto, Japan, May 2010, MOPEB053, p. 388.
- [4] I. Novitski et al., "Conceptual designs of dipole magnet for muon collider storage ring," IEEE Trans. Appl. Supercond. 21(3), (2011) 1825.
- [5] N.V. Mokhov et al., "Radiation Effects in a Muon Collider Ring and Dipole Magnet Protection," Fermilab-Conf-11-095-APC-TD (2011), PAC'11, THP085, p. 2294.
- [6] N.V. Mokhov, A.V. Van Ginneken, in Proc. ICRS-9, Tsukuba, 1999, J. Nucl. Sci. Techn., p. 172 (2000).
- [7] Y. Alexahin, E. Gianfelice-Wendt, "A 3 TeV Muon Collider Lattice Design", TUPPC041, these proceedings.
- [8] A.V. Zlobin et al., "Large-Aperture Nb₃Sn Quadrupoles for 2nd generation LHC IRs," EPAC'02, Paris, June 3-7 2002, MOPLE017, p. 2451.
- [9] M.L. Lopes et al., "Design Studies of a Dipole with Elliptical Aperture for the Muon Collider Storage Ring," THPPD037, these proceedings.
- [10] S. Russenschuck, "ROXIE - A Computer Code for the Integrated design of Accelerator Magnets," EPAC'98, Stockholm, June 1998, TUP11H, p. 2017.
- [11] V.V. Kashikhin et al., "Magnets for Interaction Regions of a 1.5×1.5 TeV Muon Collider," THPPD035, these proceedings.